

Thermorheology of living cells—impact of temperature variations on cell mechanics

Tobias R Kießling¹, Roland Stange, Josef A Käs
and Anatol W Fritsch

Institut für Experimentelle Physik I, Universität Leipzig, Leipzig, Germany
E-mail: Tobias.Kiessling@uni-leipzig.de

New Journal of Physics **15** (2013) 045026 (19pp)


Received 26 October 2012

Published 26 April 2013

Online at <http://www.njp.org/>

doi:10.1088/1367-2630/15/4/045026

Abstract. Upon temperature changes, we observe a systematic shift of creep compliance curves $J(t)$ for single living breast epithelial cells. We use a dual-beam laser trap (optical stretcher) to induce temperature jumps within milliseconds, while simultaneously measuring the mechanical response of whole cells to optical force. The cellular mechanical response was found to differ between sudden temperature changes compared to slow, long-term changes implying adaptation of cytoskeletal structure. Interpreting optically induced cell deformation as a thermorheological experiment allows us to consistently explain data on the basis of time–temperature superposition, well known from classical polymer physics. Measured time shift factors give access to the activation energy of the viscous flow of MCF-10A breast cells, which was determined to be $\approx 80 \text{ kJ mol}^{-1}$. The presented measurements highlight the fundamental role that temperature plays for the deformability of cellular matter. We propose thermorheology as a powerful concept to assess the inherent material properties of living cells and to investigate cell regulatory responses upon environmental changes.

 Online supplementary data available from stacks.iop.org/NJP/15/045026/mmedia

¹ Author to whom any correspondence should be addressed.



Content from this work may be used under the terms of the [Creative Commons Attribution 3.0 licence](http://creativecommons.org/licenses/by/3.0/). Any further distribution of this work must maintain attribution to the author(s) and the title of the work, journal citation and DOI.

Contents

1. Introduction	2
2. Methods and materials	3
2.1. Thermo-optical stretcher setup	3
2.2. Image and data processing	5
2.3. Time–temperature superposition and activation energy	6
2.4. Cell preparation	7
3. Results	7
3.1. Optical stretching is a thermorheological experiment	7
3.2. Temperature instantaneously affects cell deformability	9
3.3. Reversibility	10
3.4. Triggering thermorheological complexity	11
4. Discussion	13
Acknowledgments	16
Appendix	16
References	17

1. Introduction

Temperature plays a fundamental role in rheology. Based on the empirical observation that material functions (e.g. creep compliance) show similar shapes when measured at different temperatures, the concept of time–temperature superposition (TTS) has been widely used to study the rheological behavior of polymers for about 70 years [1, 2]. Material functions recorded at different temperatures can be rescaled to overlap, resulting in a single master curve. The said curve is frequently used to extend the experimentally accessible time or frequency range, whereas the scaling factors provide an insight into underlying molecular dynamics. TTS is expected to fail when relaxation times of structurally relevant constituents show different temperature dependences or when load bearing structures are thermally unstable within the investigated temperature range. While thermorheological measurements have been successfully used to characterize synthetic polymers, biopolymer systems as found in living cells lack systematic characterization. Only for isolated subsystems *in vitro* a distinct temperature dependence of mechanical properties has been shown for single microtubules [3], actin filament solutions [4] and in cross-linked actin/ α -actinin gels [5, 6]. Semmrich *et al* [4] recently found TTS to be applicable to rheological data of semidilute F-actin solutions, raising the question whether similar behavior could be found for F-actin networks or even whole living cells.

It is widely accepted that living cells obtain mechanical stability from a complex network of filamentous proteins, linkers and molecular motors, the cytoskeleton. In contrast to dead matter, the active biopolymer scaffold found in living cells inherently exhibits complex dynamics on the molecular level as cytoskeletal structures constantly assemble and disassemble [7]. Further, self-organized processes regulate the cytoskeletal meshwork temporally and spatially to account for cell function (e.g. migration or mitosis [8, 9]) or in response to environmental conditions (e.g. drug treatment or substrate stiffness [10, 11]). A vital goal of biophysical research is to understand how mechanical functionality emerges from microscopic interactions, forming mesoscale structures that equip a cell with its astonishing features. A common

approach is rheological studies on living cells since the mechanical properties have been identified to be crucial for many cell functions ranging from stem cell differentiation [12] to cancer progression [13]. It is an everyday experience that material properties are temperature dependent, i.e. a value for Young's modulus or viscosity is valid only for a given temperature. Surprisingly, however, during the last 50 years only a few studies have focused on how cell rheology is affected by temperature [14–19].

In living cells, virtually all structurally important parameters such as binding rates of crosslinkers [5], molecular motor activity [20, 21] or polymerization velocity of actin filaments [22] are known to be temperature sensitive and thus temperature directly affects molecular architecture and mechanical properties. While a change in temperature will instantaneously affect the flow behavior of the cytosol and cytoskeleton (e.g. via Brownian motion), a certain delay can be expected until changed cytoskeletal dynamics (e.g. changed binding rates, gene encoding efficiency or polymerization velocities) result in altered material properties on a whole cell level. Additionally, to maintain homeostasis upon a change of environmental conditions multiple cell regulatory interventions might be triggered (e.g. expression of heat-shock or cold-shock proteins), potentially further affecting cytoskeletal structure [23]. Previous studies on cell mechanics were performed at fixed temperatures or temperature was varied on long timescales only, where delayed structural and regulatory processes inside the cell are able to contribute to observed mechanical alterations. In contrast, we utilize laser-induced heating to deposit thermal energy in living cells on a millisecond timescale. To separate prompt from delayed responses, we compare cell deformation measured immediately upon a change of temperature to deformation with sufficient time for adaptation.

To probe the response of living cells to mechanical load, we use a microfluidic optical stretcher (μ OS), a laser trap that utilizes optical forces to deform single suspended cells [24, 25, 26]. Initially, we demonstrate that optical stretching actually has to be understood as a thermorheological measurement as—due to the measurement principle—force application is coupled with optical heating. Surprisingly, we find that TTS can explain the observed shift of the creep compliance curves upon sudden temperature changes. Subsequently, by slightly modifying the experimental setup, we are able to decouple optical heating from optically induced forces to verify findings from the first experiment and to investigate the reversibility of thermal effects. Finally, we demonstrate that for high temperatures as well as for temperature changes applied on long timescales not only the time axis (x -axis) but also the compliance (y -axis) has to be scaled for creating a master curve.

2. Methods and materials

2.1. Thermo-optical stretcher setup

In its standard configuration (as described in Lincoln *et al* [26]), the μ OS is a dual-beam laser trap as shown in figure 1. A square glass capillary (80 μ m inner diameter, 40 μ m wall thickness, ST8508, VitroCom, USA) is mounted perpendicular to two optical fibers (colored in yellow in figure 1) which are axially aligned facing each other at a distance of 200 μ m. To avoid reflection and diffraction effects, the glass capillary and the optical fibers were submersed in index matching gel.

Through the capillary, suspended cells can be transported to the trapping region where deformation is caused by optically induced surface stress $\sigma(t)$ [24]. Cells, first trapped at low

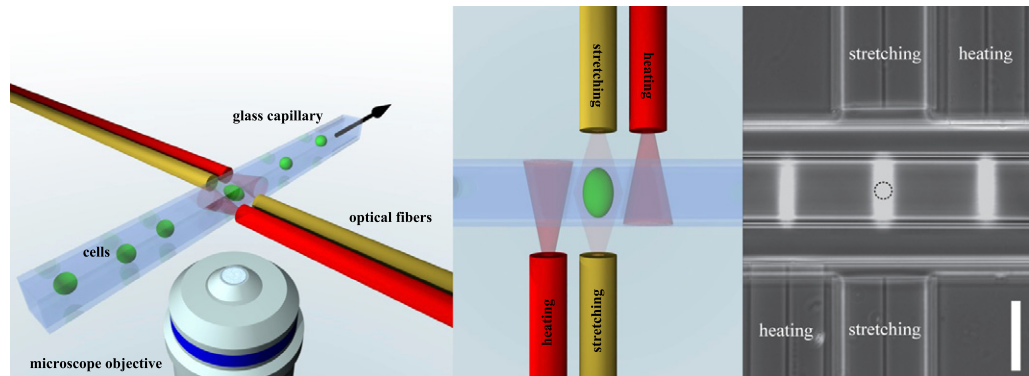


Figure 1. Modified optical stretcher setup: compared to the standard setup where a squared glass capillary is placed between two axially aligned optical fibers (yellow), forming the optical trap, the modified optical stretcher setup is extended by two heating fibers (red). Laser light, emitted from the heating fibers, does not interact with cells trapped by the standard fibers. However, by absorption of the laser light, the temperature in the measurement region can be controlled on a millisecond timescale. By applying a hydrodynamic flow in the capillary, single suspended cells can be delivered to the measurement region where cells are trapped and subsequently deformed by optical forces. Right: phase contrast image of the modified microfluidic optical stretcher setup (bar $80 \mu\text{m}$). Bright stripes are laser light emitted by the laser fibers and scattered by small particles flowing inside the glass capillary. The dashed circle depicts the size and position of a standard cell during measurement.

laser power, show creep behavior when exposed to a stepwise increased laser power P_{stretch} (video S1, available from stacks.iop.org/NJP/15/045026/mmedia). The relative deformation of the cell $\epsilon(t)$ is quantified using image analysis techniques (see section 2.2). Assuming linear viscoelastic behavior, the observed deformation directly translates into a creep compliance $J(t)$ via

$$J(t) = \frac{\epsilon(t)}{\sigma_0}. \quad (1)$$

Herein, the optically induced stress $\sigma_0(t)$ depends linearly on the applied laser power P_{stretch} [24, 25]. In our setup, cells were delivered out of a reservoir to the measurement region via a pressure-driven pump system connected to the capillary. The whole measurement procedure including the pump system, laser and temperature control was automatically executed by custom-made LabVIEW software (National Instruments, Austin, TX). As previously shown by several authors [27–29], optical stretching is unavoidably accompanied by a laser-induced temperature rise of cell medium and cells on a timescale of several milliseconds. Its impact on cell deformability, however, has not been investigated yet but will be clarified throughout this work.

To study temperature-dependent cell rheology on short and long timescales, we extended the standard setup by two slight modifications. Firstly, to control the temperature of the whole setup (including the cell container), we designed a custom-made aluminum sample holder, steadily flushed by temperate water from a thermostat (F10, Julabo, Germany). The thermostat

was looped back by an external thermosensor positioned close to the measurement region, guaranteeing a stable setup temperature during experiments and stable temperature changes within approximately 20 min (shown in figure 6(D)). Secondly, to realize temperature jumps within a millisecond range we added two optical fibers positioned at a distance of 110 μm to the trapping region (colored in red in figure 1). When these fibers emit laser light of 1064 nm, the cell medium around the measurement region is quickly heated up, without direct exposition of trapped cells to laser light. As the expected temperature rise in the measurement region strongly depends on the distance of the laser fibers, we aimed at minimizing this distance by etching the heating laser fibers (standard HI-1060 single mode fibers) from 125 μm down to a diameter of 80 μm using hydrofluoric acid.

To calibrate the temperature rise in the measurement region for both stretch and heating laser emission, we used a temperature sensitive fluorescent dye, similar to the procedure described in [27]. In brief, as the temperature indicator we chose the fluorescent dye Rhodamine B (Sigma-Aldrich, St. Louis, Missouri), since it has high temperature sensitivity in the range of 0–120 °C [30]. To obtain temperature information for a large field of view, we used an Axioobserver.Z1 in combination with a 10 \times objective (Carl Zeiss, Jena, Germany). The dye solution was prepared from Rhodamine B (0.1 mM) in carbonate buffer (20 mM), loaded into the μOS setup and calibrated by measuring the fluorescence intensity at different setup temperatures. For determining the laser-induced temperature rise inside the glass capillary, we took the average of six independent measurements performed at six different setup temperatures between 15 and 40 °C, to make sure that neither the setup temperature nor other nonlinearities of the Rhodamine B dye significantly affected our results. For the heating lasers, we measured an increase of temperature of $\Delta T_h = 7 \text{ }^\circ\text{C W}^{-1}$ (per fiber) in the measurement region and for the stretch lasers an increase of $\Delta T_s = 26 \text{ }^\circ\text{C W}^{-1}$ (per fiber) (figure 2). Note that all values of laser powers presented throughout the paper are reported per fiber of either stretch or heat laser pair.

2.2. Image and data processing

The extraction of quantitative values from single-cell experiments comprises the digital processing of image stacks, recorded at 30 frames per second by video phase contrast microscopy. An edge detection algorithm, as proposed by Lincoln *et al* [26], was implemented in MATLAB (The Mathworks, USA), detecting the outer edge of every measured cell with subpixel accuracy. Subsequently, we applied a shape-tracking algorithm on obtained contour data to minimize the influence of small rotations around the optical axis of the microscope. The rotation corrected data were then used to determine the deformation along the laser beam. In supplementary video S1 (available from stacks.iop.org/NJP/15/045026/mmedia), an image sequence recorded during a stretch experiment is shown, together with the applied laser pattern and the detected cell deformation. To demonstrate the working principle of the rotation correction, a cell showing a clear rotation is presented in video S1. Our shape-tracking algorithm is able to account for cells showing small rotations around the optical axis of the microscope (see the green bar in video S1). However, rotations around any other axis (e.g. the axis of the laser beam) principally hinder accurate detection of the optically induced deformation, thus those cells were excluded from further evaluation. The cell deformations were quantified in terms of relative deformation, calculated as $\epsilon(t) = (L_{\parallel}(t) - L_{\parallel}(0))/L_{\parallel}(0)$, where $\epsilon(t)$ is the relative deformation, $L_{\parallel}(t)$ is the measured length of the cell along the laser axis at time t and $L_{\parallel}(0)$ is the length of the cell before starting the stretch experiment.

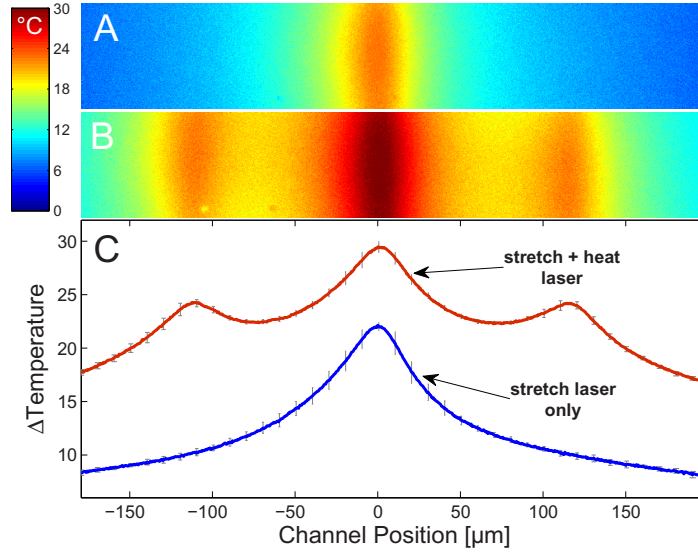


Figure 2. Spatial temperature distribution in the capillary of the modified optical stretcher. (A) Color-coded temperature distribution in the microfluidic channel for a stretch laser emission of 800 mW per fiber and no heating laser emission. (B) Temperature distribution during a stretch laser emission of 800 mW and a heating laser emission of 1000 mW (both per fiber). (C) Line average of the measured distributions of panels (A) (lower curve) and (B) (upper curve). When heat lasers are activated the temperature in the trapping region increases by $\sim 7 \text{ K W}^{-1}$ of heating laser power in each fiber (channel position = 0).

2.3. Time–temperature superposition and activation energy

Phenomenologically motivated and supported by basic polymer models (Rouse, Zimm, Williams, Landel, Ferry), the influence of temperature on the rheology of a broad class of polymers can be described by TTS, for creep experiments given by

$$J(t, T_{\text{ref}}) = \frac{J_i(t/a_{T_i}, T_i)}{b_{T_i}}. \quad (2)$$

Creep compliance curves J_i measured at an arbitrary temperature T_i can be shifted to overlap with a measurement J taken at a reference temperature T_{ref} by scaling time with a time shift factor a_{T_i} and the whole creep function by a modulus shift factor b_{T_i} [31]. For simple, thermally stable polymeric systems, b_{T_i} is expected to be not or only slightly temperature dependent, while the influence of temperature is mainly expressed by a rescaling of the time axis via a_{T_i} . In the literature therefore, materials following equation (2) are often called thermorheologically simple if all $J_i(t)$ superimpose just by applying a temperature-dependent time shift factor a_{T_i} [32].

Considering viscous flow as a thermally activated process, the temperature dependence of a_{T_i} is of special interest to polymer physics as it provides information on the activation energy of molecular movement [32]. In the simplest case, a_{T_i} shows an Arrhenius dependency [31]

$$\log(a_{T_i}) = \frac{E_A}{R} \left(\frac{1}{T_i} - \frac{1}{T_{\text{ref}}} \right), \quad (3)$$

where E_A is the (constant) activation energy and R is the universal gas constant. However, for glassy materials (which cells are frequently speculated to be [33–35]) in the vicinity of the glass transition temperature T_g , a_{T_i} is normally observed to not obey Arrhenius behavior as activation energy becomes a function of temperature [31, 32]. Then, the temperature dependence of a_{T_i} above T_g is often successfully described by the William–Landel–Ferry (WLF) equation

$$\log(a_{T_i}) = \frac{-C_1(T_i - T_{\text{ref}})}{C_2 + (T_i - T_{\text{ref}})}, \quad (4)$$

where C_1 and C_2 are empirical factors [2].

We implemented a custom-made algorithm to construct a master curve from mean creep compliance curves, measured at different temperatures. After selecting a reference curve, all the other curves were scaled according to equation (2), while scaling factors a_{T_i} and b_{T_i} were systematically varied to minimize the error of the overlap. To account for the stochastic nature of cell-rheological data, the procedure was repeated for various binning values, reference temperatures and random subsets of cells to construct the mean curves while the reported values for a_{T_i} , b_{T_i} and E_A (equation (3)) were found to be restored in most cases. Due to the lack of a clear curvature in the data when plotting a_{T_i} over T_{eff} (e.g. in figure 7(A)), fitting values for equation (4) (the WLF equation) were found to be sensitive to statistical variation. However, the ratio between the constants C_2 and C_1 was widely conserved and found to be close to a value of 10.

2.4. Cell preparation

MCF-10A cells (CRL-10317), a non-tumorigenic epithelial cell line, were obtained from American Type Culture Collection (ATCC, Manassas, VA). MCF-10A were maintained in a 1:1 mixture of Dulbecco's modified Eagle's medium and Ham's F12 medium, supplemented with 5% horse serum, 20 ng ml⁻¹ epidermal growth factor, 10 μ g ml⁻¹ insulin, 100 ng ml⁻¹ cholera toxin, 500 ng ml⁻¹ hydrocortisone and 100 U ml⁻¹ penicillin/streptomycin. Prior to measurements, cells cultured in 25 cm² flasks were detached by application of 1 ml 0.025% trypsin–EDTA solution, resuspended in 3 ml of culture medium and centrifuged at 100g for 4 min. Finally, single cells were resuspended in culture medium to a concentration of about 5×10^5 cells ml⁻¹ and loaded into the μ OS.

3. Results

3.1. Optical stretching is a thermorheological experiment

In the μ OS (and in any other optical trap) a higher laser power produces higher optical forces, while—due to light absorption in aqueous medium—simultaneously raising the temperature in the trapping region. When assuming small deformations ($\epsilon(t) \propto \sigma_0$), then creep compliance $J(t)$ is independent of the applied force (equation (1)). Consequently, instantaneous effects of temperature changes on optically induced cell deformability can be investigated experimentally by comparing creep compliance curves, obtained for different stretch laser powers.

In a standard μ OS setup, creep experiments were sequentially performed on single cells with a random stretch laser power P_{stretch} for each experiment (figure 3(C)). This ensures that the final average curves for different laser powers (figure 3(A)) comprise cells that were measured

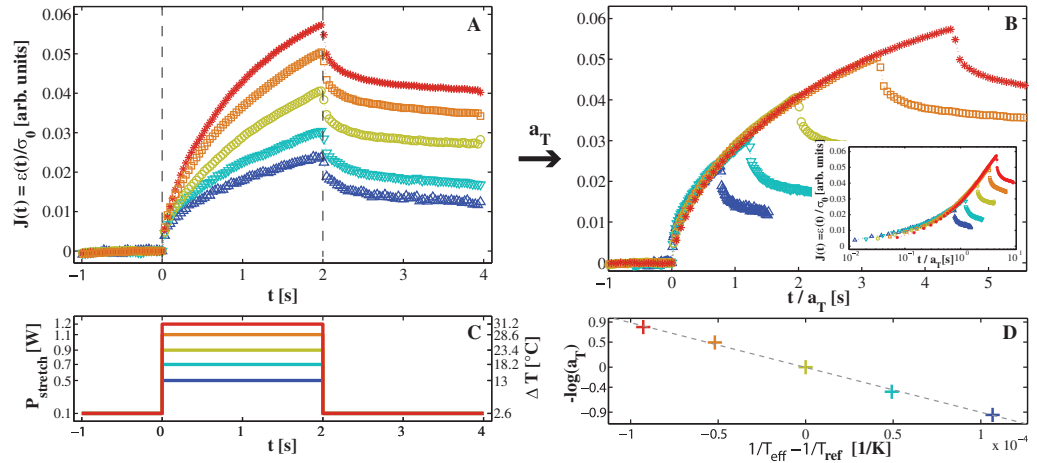


Figure 3. At a setup temperature of $T_{\text{setup}} = 15^\circ\text{C}$, creep curves of living cells were sequentially probed with varying peak values for the stretch laser power P_{stretch} . (A) Mean creep curves $J(t)$ of 137 cells, binned by applied stretch laser power. (B) Same creep compliance curves as shown in (A), individually scaled with a time shift factor a_{T_i} to overlap with the measurement at $T_{\text{ref}} = 38.4^\circ\text{C}$ (green circles). (C) Applied stretch patterns, randomly chosen for each individual cell. (D) Arrhenius plot of time shift factors a_{T_i} . The gray dashed line represents a fit of equation (3) to the data. For scaling factors and visualization of shifting see table A.1 and video S2 (available from stacks.iop.org/NJP/15/045026/mmedia).

at various time points of the whole experiment. Hence, possible long-term dependences of cell deformability, for example as reported in [33], should cancel out.

In figure 3(A), average creep curves of 137 cells are displayed, binned by applied laser power P_{stretch} . Creep curves for different stresses ($\sigma_0 \propto P_{\text{stretch}}$) do not overlap as would be expected for a temperature-independent viscoelastic linear material, but rather show significant bigger compliance for higher laser powers. We state that the apparent drop of stiffness as seen in figure 3(A) is caused by laser-induced heating during the step stress experiment. This hypothesis is supported by the observation that creep compliance curves for different laser powers overlap surprisingly well by scaling exclusively with a_{T_i} (figure 3(B)).

In this experiment, each laser power P_{stretch} can be translated to an effective temperature T_{eff} via $T_{\text{eff}} = T_{\text{setup}} + P_{\text{stretch}} \Delta T_s$, including the setup temperature T_{setup} (constantly held at 15°C throughout the whole measurement) and a laser-induced heating of $\Delta T_s = 26^\circ\text{C W}^{-1}$ determined by calibration (see section 2.1). The time shift factors a_{T_i} used in figure 3(B) to scale the creep curves are plotted in figure 3(D) in an Arrhenius plot.

Hitherto no appropriate value for the activation energy E_A or the glass transition temperature T_g has been proposed for whole living cells. From our experimental data it cannot be decided whether the observed dependency displayed in figure 3(D) follows Arrhenius behavior (equation (3)) or rather represents a flat version of the WLF equation (equation (4)). When assuming Arrhenius behavior, the activation energy for the viscous flow of living suspended MCF-10A cells turns out to be $E_A \approx 74 \text{ kJ mol}^{-1}$. In contrast, the equivalent activation energy of pure water at $T = 37^\circ\text{C}$ is much lower with $E_A^{\text{water}} \approx 17 \text{ kJ mol}^{-1}$ [36]. Thus, it is unlikely that we measure the temperature dependence of the free surrounding aqueous medium only. It would

be interesting to compare E_A to values for the activation energy of reconstituted cell biopolymers; however, to our knowledge there are no such values available in the literature up to now. Values of standard polymer melts like polystyrene are unintuitive as comparison since they are measured at temperatures of hundreds of celsius (e.g. polystyrene $E_A = 59 \text{ kJ mol}^{-1}$ [37]). Due to the aforementioned coupling of heat and force in the optical stretcher, we had to make an assumption on how the creep compliance scales with the applied force, i.e. we assumed the simplest case of linear viscoelasticity. However, it is important to note that we do not state that cellular material is fully linear viscoelastic but rather that laser-induced heating can mostly explain the apparent increase of compliance for higher laser powers, shown in figure 3(A). In the next section, we modify our experimental setup rendering the need for assuming linear behavior superfluous.

3.2. Temperature instantaneously affects cell deformability

The observed systematic shift of $J(t)$ (figure 3(A)) can be explained as temperature induced but could also arise from a nonlinear response to applied stress, e.g. shear thinning. In order to exclude nonlinear viscoelastic effects, it is necessary to measure cells with the same stress $\sigma_0(t)$ but at different temperatures T_{eff} .

To realize an experiment where the applied stress can be kept constant while temperature changes can be independently applied on a short timescale, we further exploit the effect of laser-induced heating. We designed a modified μOS setup, extended by two optical fibers (colored in red in figure 1), further denoted as heating fibers. By laser emission of the heating fibers, trapped cells can be heated on a millisecond timescale without being directly illuminated. The applied stress σ_0 , exclusively determined by emission of the stretch fibers, however can be kept constant. Hence, heat generation and force application are partially decoupled in the modified μOS setup.

We measured cells with a fixed stretch laser power of $P_{\text{stretch}} = 700 \text{ mW}$ per fiber (figure 4(A)). One second before the stretch started, we activated the heating laser to randomly emit a power of P_{heat} between 0 and 1700 mW per fiber, causing a sudden change of temperature in the measurement region (figure 4(B)). Similar to the situation above, an effective temperature can be calculated for each single experiment via $T_{\text{eff}} = T_{\text{setup}} + P_{\text{stretch}} \Delta T_s + P_{\text{heat}} \Delta T_h$, including the temperature rise caused by emission of the heating fibers. A calibration measurement (figure 2) revealed a local temperature increase of $\Delta T_h \approx 7^\circ\text{C W}^{-1}$ (per fiber) in the measurement region (see methods and figure 2).

Creep compliance curves of cells do not overlap when measured with the same stress $\sigma_0(t)$ but different heating laser values P_{heat} . This confirms our hypothesis that cell deformability is strongly temperature dependent as effects of different forces can now be excluded. In figure 4(C), we demonstrate that measured curves again superimpose by only varying time shift factors a_{T_i} while b_{T_i} can be set to a constant value. Similar to the experiment with different stretch laser powers (figure 3), cells exhibit thermorheologically simple behavior. Fitting equation (3) (Arrhenius) leads to an activation energy of $E_A \approx 75 \text{ kJ mol}^{-1}$, a similar value as measured before in section 3.1.

With this experiment, we can reasonably argue that temperature instantaneously affects the deformability of single suspended cells. As nonlinear viscoelastic effects can now be excluded, laser-induced heating is identified as the dominant factor, responsible for the apparent drop of stiffness with increasing stretch laser power (figure 3(A)).

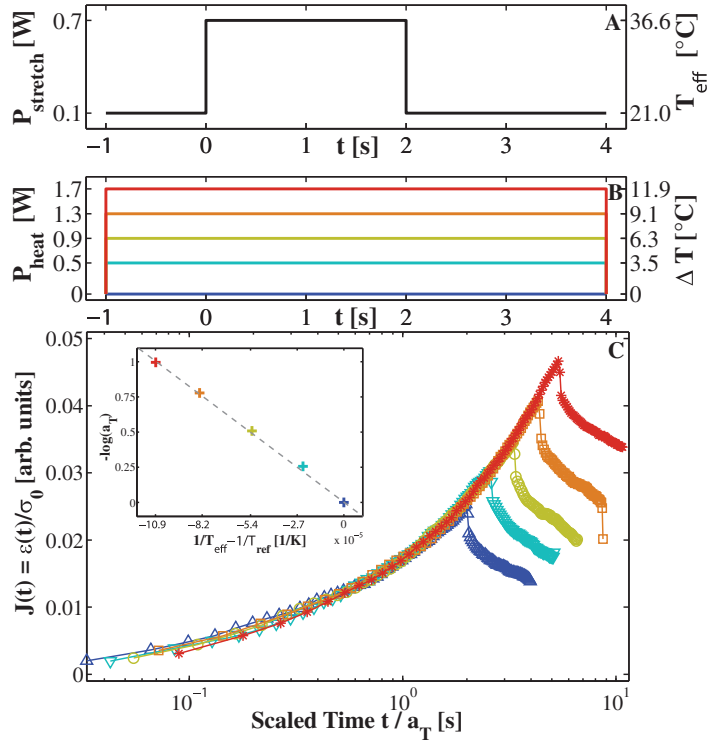


Figure 4. At a setup temperature of $T_{\text{setup}} = 18.4^\circ\text{C}$, 207 cells were stretched with the same stretch laser pattern P_{stretch} shown in (A). (B) For each single cell, a random heating laser pattern P_{heat} was chosen, leading to an instantaneous increase of temperature ΔT in the measurement region. (C) Mean creep curves $J(t)$, binned by applied heat laser power and scaled by a_{T_i} to overlap. The optically induced stress was the same for all measured cells, while the individual temperature T_{eff} differed for each stretch experiment (inset: Arrhenius plot of time shift factors a_{T_i} . The gray dashed line represents a fit of equation (3) to the data). For scaling factors and visualization of shifting see table A.2 and video S3 (available from stacks.iop.org/NJP/15/045026/mmedia).

3.3. Reversibility

A necessary prerequisite for the applicability of TTS is the reversibility of temperature effects. As shown in the measurements above, creep rates were increased when temperature was raised. Consequently, a reduction of temperature should lead to a reduction of creep rates. At a setup temperature of $T_{\text{setup}} = 23^\circ\text{C}$, cells were measured with a constant stretch laser power $P_{\text{stretch}} = 600\text{ mW}$ per fiber for 6 s (figure 5(A)). Within these 6 s, we activated the heat lasers for 2 s, emitting a random power P_{heat} between 0 and 1500 mW per fiber (figure 5(B)).

Figure 5(C) shows creep compliance curves for 843 cells, binned by applied heat laser power P_{heat} . At $t = 2\text{ s}$, creep rates instantaneously increase upon activation of heat lasers. At $t = 4\text{ s}$, heat lasers are switched off and creep rates return back to baseline levels, comparable to cells where no temperature rise has been applied.

This experiment demonstrates that creep rates directly depend on temperature. However, as living cells are active systems and thermally fragile it is clear that reversibility and TTS can only

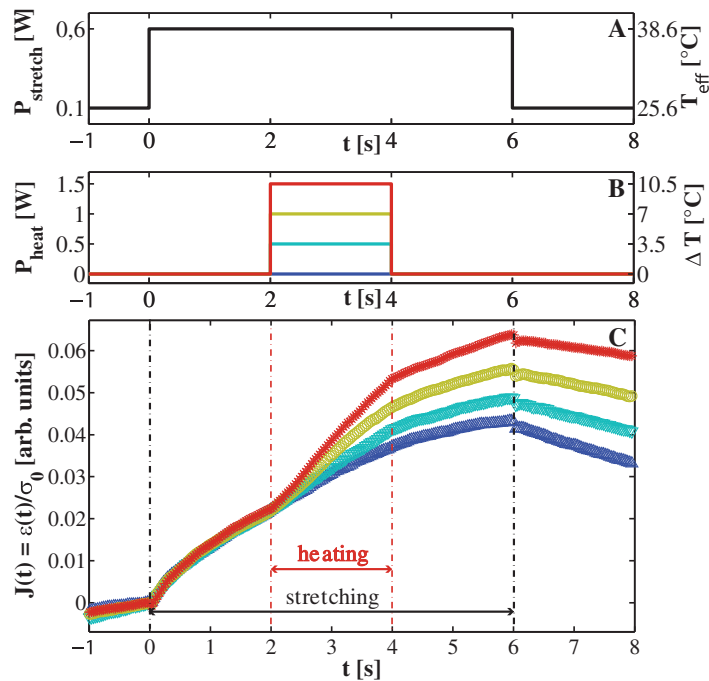


Figure 5. Temperature variation during the stretch experiments. (A) At a setup temperature of 23 °C, 843 cells were measured for 6 s with a constant stretch power of 600 mW per fiber. (B) During the stretch at $t = 2$ s, the heat lasers were activated for 2 s with a randomly chosen P_{heat} , causing a temperature increase of ΔT of the probed cell. (C) Mean creep compliance $J(t)$, binned by the applied heating laser power P_{heat} . The higher the temperature increase, the higher the increase in deformation rate at $t = 2$ s. After deactivation of the heat laser at $t = 4$ s, deformation rates are reduced again.

be valid within certain limits. The applicability of TTS naturally cannot be expected *a priori* for timescales where regulatory processes actively alter the cytoskeleton as well as for temperatures where the structure of load-bearing proteins is irreversibly altered.

3.4. Triggering thermorheological complexity

In previous sections, T_{setup} was kept constant while—using laser-induced heating—sudden effects of temperature changes were studied. To assess how cellular material changes with temperature over a longer period, we performed creep experiments at different setup temperatures T_{setup} , such that cells had several minutes and hours to adapt to the new ambient temperature before being optically trapped and deformed.

In the beginning, the setup temperature was set to 37 °C and ≈ 200 cells were measured within approximately 3 h. Subsequently, the setup was cooled down to 25 and 15 °C where measurements were repeated with approximately the same amount of cells and the same range of stretch laser power P_{stretch} , randomly chosen between 600 and 1300 mW per fiber (figure 6(C)/(D)). Each cooling step required about 20–25 min until the whole setup was thermally equilibrated (gray points in figure 6(D)). Cells measured during temperature transition were excluded from further evaluation.

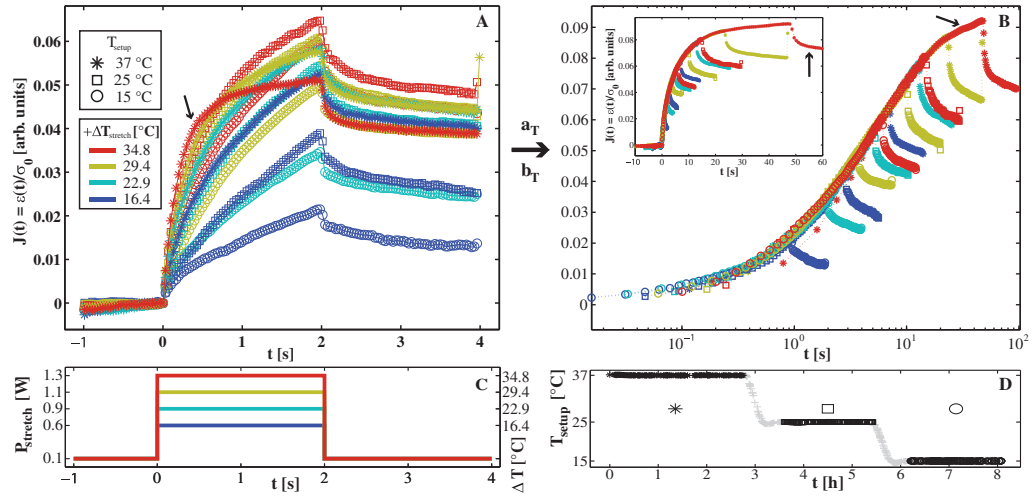


Figure 6. Long-term effects of temperature. (A) Mean creep curves $J(t)$, binned by applied stretch laser power and setup temperature (B) scaled by a_{T_i} and b_{T_i} to overlap (inset: linear representation). To illustrate the scaling procedure the creep curve for the cells at the highest temperature is marked with an arrow. For a more detailed visualization of shifting see video S4 (available from stacks.iop.org/NJP/15/045026/mmedia). (C) Applied stretch laser pattern $P_{stretch}$, randomly chosen for each cell. (D) At three different setup temperatures T_{setup} (\star : 37 °C; \square : 25 °C; \circ : 15 °C), cells were measured over a time course of 8 h. Cells measured during cooling (gray crosses) were excluded from evaluation.

In figures 6(A) and (B), we demonstrate that the creep curves can be scaled according to equation (2) to overlap in a single master curve. Used time shift factors a_{T_i} and modulus shift factors b_{T_i} are plotted in figure 7 and listed in table A.3: in contrast to the previous experiments, the modulus shift factor b_{T_i} can no longer be kept constant. Creep curves obtained at $T_{setup} = 15^\circ\text{C}$ still behave thermorheologically simple, as the corresponding values for b_{T_i} are equal for all stretch laser powers $P_{stretch}$ (marked as circles in figures 6 and 7). However, curves obtained at $T_{setup} = 25^\circ$ have to be rescaled by a different value for b_{T_i} to superpose with the measurements at 15°C . The same holds true for measurements carried out at $T_{setup} = 37^\circ\text{C}$. Despite the fact that several creep curves were obtained at the same effective temperature T_{eff} , a different value for b_{T_i} is required to make curves superpose when the setup temperature T_{setup} was changed in between. Apparently, the occurrence of thermorheological complexity is associated with the fact that cells had time to adapt to the changed setup temperature. For the same T_{eff} , cells appear stiffer when measured at higher T_{setup} .

As shown in figure 7(B), thermorheologically complex behavior generally occurs for all creep curves measured at effective temperatures T_{eff} higher than a critical temperature $T_{crit} \approx 52^\circ\text{C}$: a non-constant modulus shift factor b_{T_i} is necessary for sufficient superposition of curves, regardless of whether T_{setup} was changed in between or not. On long timescales, we proposed cellular adaptation to explain the occurrence of thermorheological complexity. On short timescales, thermal fragility of load bearing structures in the cell appears to be a more plausible explanation for the variation of b_{T_i} for $T_{eff} > T_{crit}$.

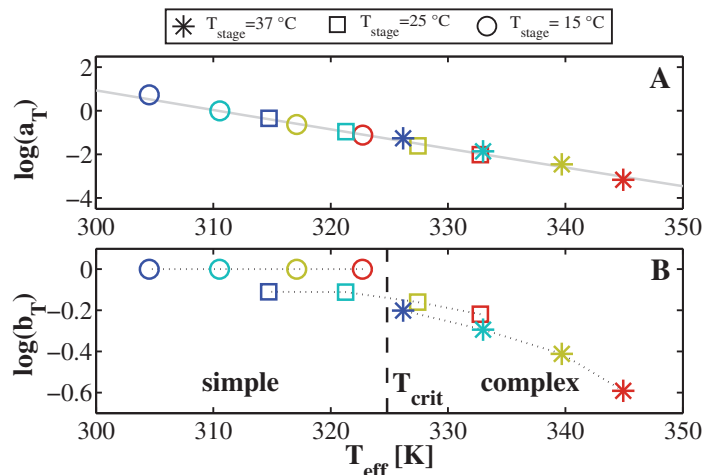


Figure 7. Scaling factors a_{T_i} and b_{T_i} used in figure 6 (\star : 37°C ; \square : 25°C ; \circ : 15°C). (A) Plot of time shift factors a_{T_i} over effective temperature T_{eff} . The gray dashed line represents a fit of equation (3) to the data ($E_A = 79 \text{ kJ mol}^{-1}$). (B) Modulus shift factors b_{T_i} over T_{eff} . Upon a change of the setup temperature T_{setup} (duration ≥ 20 min) or for $T_{\text{eff}} > T_{\text{crit}}$, the value for b_{T_i} can no longer be kept constant, but must be adjusted for sufficient overlapping of $J(t)$. For the same T_{eff} , cells are stiffer when stored at higher T_{setup} . For scaling factors, see table A.3. Colors indicate different stretch laserpowers (compare to figure 6C).

4. Discussion

We propose TTS (equation (2)), a widely used concept in polymer physics, as the leading term to rationalize the observed temperature dependence of the creep compliance $J(t)$ of cells: for sudden temperature changes that do not exceed a critical temperature T_{crit} , we observe thermorheologically simple behavior, meaning that $J(t, T)$ superpose by only scaling with a time shift factor a_{T_i} . However, temperature changes on timescales of several minutes and hours or above T_{crit} demand for additional scaling with a modulus shift factor b_{T_i} .

Considering the complex dynamics of myriads of biochemically and physically diverse constituents, the extension of scaling concepts derived from rather simple synthetic polymers to the rheology of whole living cells is a remarkable and unexpected feature. A major assumption, often denoted as necessary for the applicability of TTS, is that relaxation times of all load-bearing structures exhibit the same temperature dependence [31]. This appears to be rather unlikely seeing that the cytosol comprises an incredible number of structurally different proteins that potentially contribute to the observed deformation upon mechanical load. A possible explanation for the apparent thermal homogeneity of a cell's compound material could be given by the fact that the cytoskeletal network is a tightly crosslinked structure. From miscible polymer blends, it is known that the presence of strong bonding can lead to a coupling of the dynamic responses of the component chains such that *dynamic homogeneity* and the successful application of TTS would be restored [38]. In turn, this would mean that cytoskeletal drugs targeting the coupling of load bearing structures in the cell should be able to destroy the dynamic coupling. Further, cell types with inherently lower connectivity of cytoskeletal components should violate TTS, as individual relaxation times of load bearing structures and processes must be assumed to depend differently on temperature. The observed simple TTS dependency could

be also explained by postulating that optical cell stretching is mainly governed by a single thermally activated process that dominates cellular response. With respect to the often reported glassy character of cellular matter [33–35], one could speculate, for example, about a glass transition of one of the compounds, e.g. the cytosol, dominating the observed cell response by stretching the time scale and thus creating the apparent dynamic homogeneity. Similar to classic polymers, thermorheological measurements on living cells could be a promising approach to discern the role of different compounds and to investigate changes of the cytoskeletal structure.

In the framework of TTS, the time shift factor a_{T_i} accounts for the inherent acceleration of molecular dynamics at higher temperatures. For a viscoelastic material, a_{T_i} can be associated with a change of the viscosity, while the modulus shift factor b_{T_i} accounts for changes of the elastic part of the material [32]. The apparent need for a non-constant b_{T_i} or general poor overlapping of shifted curves (thermorheological complexity) can be linked to structural changes on a molecular level [39]. In our measurements, when temperature is changed on short timescales we observe a monotonic decrease of the modulus shift factor b_{T_i} only for temperatures higher than T_{crit} (figure 7(B)). Below T_{crit} , b_{T_i} can be set to a constant, meaning that the impact of a rapid temperature change is solely captured by the time shift factor a_{T_i} . Thus, our data imply that temperature variations on short timescales mainly affect the viscous part of the viscoelastic cell material, i.e. cells are more fluid at higher temperatures. Rapid temperature changes above T_{crit} , however, demand for additional scaling by b_{T_i} to achieve overlap of measured curves. It is conceivable that above a threshold temperature structurally important macromolecules significantly alter or even denature as biopolymers in living cells can reasonably be denoted as thermally fragile. We propose that those alterations on a molecular level directly impact creep behavior on a whole cell level, reflected in non-constant values for b_{T_i} above T_{crit} . Indicated by studies on hyperthermia, where a critical temperature is a function of heating time and temperature history [40, 41], it is likely that our reported T_{crit} is valid for the heating time in our experiments only and might change e.g. for longer exposure to elevated temperature.

In the case where cells have sufficient time for adaptation to ambient temperature, we expect slower self-regulated processes such as delayed structural responses [42] or active cell regulation to contribute to alterations of load bearing structures on a whole cell level. We find that temperature changes on long timescales affect both the elastic as well as the viscous part of the viscoelastic cell material. When T_{setup} is slowly increased, the modulus shift factor b_{T_i} decreases, meaning that cells appear more elastic (i.e. bigger Young's modulus) when stored at higher setup temperatures (figure 7(B)). For the viscous part, again we find that cells continuously become more fluid at higher temperatures regardless of whether temperature changes were applied rapidly or on a long timescale (figure 7(A)).

These counter-acting effects—increase of elasticity and drop of viscosity—are qualitatively in accordance with a recent study [18], where oscillatory atomic force microscopic (AFM) measurements were used to measure storage (G') and loss modulus (G'') of adhered human alveolar epithelial cells. Sunyer *et al* [18] report a drop of viscosity for a long-term temperature increase of untreated cells (see tables 1 and 2 in [18]). Simultaneously, an increase of elasticity was observed, which was associated with increased activity of myosin motors and thereby generated prestress via traction force microscopy. We therefore assume that molecular-motor generated prestress, but also delayed physical responses, for example arising from a new adjustment of the chemical equilibrium of weak bonds in the cytoskeleton [42], could contribute to the observed variations of b_{T_i} below T_{crit} for slow temperature changes.

Our observed increase of elasticity for higher setup temperature appears at first glance to be contrary to recently published measurements using force-indentation AFM-measurements.

Rico *et al* [19] report cell softening with increasing temperature on barely attached, monocytic cells with spherical geometry. We note that force-indentation measurements by nature do not directly provide access to G' and G'' , but determine the Young's modulus via indentation depth at constant force [19], while a drastic drop of viscosity (such as observed for detached cells in our measurements) can easily overlay a possible increase of elasticity. Also in our measurements cells are more deformable at higher temperatures and could thus be denoted as softer. However, analysis of our measurements in terms of TTS suggests that increased deformability is rather due to a drop of viscosity than to a drop of elasticity. This illustrates a great advantage of thermorheological analysis of complex materials as insights can be gained independently of a viscoelastic model, i.e. without making any assumptions about the explicit functional form of the creep compliance. Since we observe identical behavior for a_{T_i} for slow and rapid temperature variations (figure 7(A)), we can assume that the temperature-induced decrease of viscosity is an inherent property of the cell material, while an increase of elasticity appears to be more cell-regulated as it only emerges when cells were allowed to adjust to a new temperature.

It has to be noted that superposition of $J(t)$ does not automatically imply superposition for other, frequency-dependent material functions [43]. Thus, it would be interesting to know whether TTS is also valid for frequency-dependent thermorheological measurements on living cells. Those could be realized, for example, by combining laser-induced heating and AFM where oscillatory measurements could be performed while simultaneously switching the temperature. According to TTS, the frequency-dependent response should be shifted instantaneously upon temperature change, while a change in the shape of the relaxation spectrum would arise from different temperature dependences of the components.

While temperature jumps investigated in this study might be considered as out of the typical physiological range, we believe that systematic thermorheological studies can contribute to a better understanding of cells as a living compound material. As a simple estimate the change of the compound shear viscosity η of cells can be derived from the Rouse model as $a_{T_i} \propto \eta(T_i)/\eta(T_{\text{ref}})$ to be of the order of 10% per kelvin around 37 °C. A change in viscosity has direct impacts on cell physics, which is dominated by Brownian motion and activated processes [42]. By directly affecting an important transport mechanism, a changed diffusivity for example can be expected to have an unspecific impact on various cell functions and could play a role in various temperature-sensitive biological functions, ranging from gene expression [44] or cell shape oscillation of cultured cells [45], protein folding [46] and mitosis [47], even up to the temperature-dependent sex determination observed in several species [48, 49].

The presented experiments were performed in a μ OS in which—due to the measurement principle—optical force and optically induced heating are inherently coupled. As a simplification, we assumed an instant temperature increase upon a rise of laser power. However, during optical stretching, temperature is a function of time where at the beginning of the step stress, temperature rises steeply [27]. As demonstrated here, temperature instantaneously affects cell deformability such that a significant temperature rise during the first milliseconds of the step-stress experiment is reflected in the observed creep function. Optical stretcher experiments, therefore, actually cannot be treated as isothermal experiments, which has several implications for their interpretation. Firstly, this could explain why results from optical stretcher measurements were reported to deviate from results obtained with other cell rheological techniques where power law behavior ($J(t) = At^a$) is widely observed [33, 50]. Secondly, Maloney *et al* [33] recently proposed an offset power law $J(t) = At^a + B$ (for fitting creep curves obtained in a μ OS) with an offset parameter B which has not been reported by other

groups. The initial rise of temperature during the measurement can naturally explain the necessity for the additional constant B , particularly with regard to the observation that B was found to be ≤ 0 . Also, the reported discrepancy between cell deformation upon stretching and recovery after stress release [33] can be explained, as laser power, and therefore temperature, is lowered during creep relaxation.

We demonstrated the concept of TTS for living cells, using MCF-10A breast epithelial cells as a model system. We propose thermorheology as a powerful concept for cell-rheological studies, especially since no assumptions about the explicit functional form of the observed material function are necessary. Our measurements demonstrate that the mechanical response of cellular material strongly depends on temperature and differs between temperature changes on long and short timescales. This insight could be important for other studies on cells and cell mechanics, especially for methods based on optical force application.

Acknowledgments

We thank Klaus Kroy for helpful discussions and Steve Pawlizak and Tina Händler for help with 3D rendering. Financial support was provided by the Deutsche Forschungsgemeinschaft within the Graduate School BuildMoNa, the European structural funds ESF and the Sächsische Aufbau Bank SAB.

Appendix

A.1. Data tables

In tables A.1–A.3, the row with italic values were used as a reference curve for TTS and is the one closest to 37 °C.

Table A.1. Corresponding to figure 3. Arrhenius fit: $E_A = 74.3 \text{ kJ mol}^{-1}$; WLF fit: $C_1 = 14.26$, $C_2 = 154.34$, $C_2/C_1 = 10.82$.

P_{stretch} (W)	T_{setup} (°C)	T_{eff} (°C)	a_T	b_T
0.52	15	28.31	2.593	1
0.72	15	33.62	1.634	1
<i>0.90</i>	<i>15</i>	<i>38.32</i>	<i>1.000</i>	<i>1</i>
1.09	15	43.42	0.611	1
1.26	15	47.57	0.449	1

Table A.2. Corresponding to figure 4. Arrhenius fit: $E_A = 75.2 \text{ kJ mol}^{-1}$; WLF fit: $C_1 = 8.31$, $C_2 = 81.16$, $C_2/C_1 = 9.77$.

P_{stretch} (W)	P_{heat} (W)	T_{setup} (°C)	T_{eff} (°C)	a_T	b_T
0.7	<i>0.13</i>	<i>18.4</i>	<i>37.50</i>	<i>1.000</i>	<i>1</i>
0.7	0.46	18.4	39.80	0.773	1
0.7	0.87	18.4	42.72	0.601	1
0.7	1.31	18.4	45.77	0.459	1
0.7	1.68	18.4	48.37	0.369	1

Table A.3. Corresponding to figure 6. Arrhenius fit: $E_A = 79.8 \text{ kJ mol}^{-1}$; WLF fit: $C_1 = 153.42$, $C_2 = 1711.48$, $C_2/C_1 = 11.16$.

P_{stretch} (W)	T_{setup} ($^{\circ}\text{C}$)	T_{eff} ($^{\circ}\text{C}$)	a_T	b_T
0.63	15	31.41	2.106	1
0.88	15	37.41	1.000	1
1.13	15	43.97	0.535	1
1.33	15	49.59	0.327	1
0.63	25	41.59	0.703	0.895
0.88	25	48.14	0.342	0.895
1.13	25	54.28	0.198	0.852
1.33	25	59.61	0.133	0.803
0.63	37	53.02	0.282	0.817
0.88	37	59.84	0.155	0.744
1.13	37	66.55	0.085	0.662
1.33	37	71.79	0.041	0.553

References

- [1] Leaderman H 1943 *Elastic and Creep Properties of Filamentous Materials and Other High Polymers* (Washington, DC: Textile Foundation) pp 238–51
- [2] Williams M L, Landel R F and Ferry J D 1955 The temperature dependence of relaxation mechanisms in amorphous polymers and other glass-forming liquids *J. Am. Chem. Soc.* **77** 3701–7
- [3] Kis A *et al* 2002 Nanomechanics of microtubules *Phys. Rev. Lett.* **89** 248101
- [4] Semmrich C *et al* 2007 Glass transition and rheological redundancy in F-actin solutions *Proc. Natl Acad. Sci. USA* **104** 20199–203
- [5] Xu J, Wirtz D and Pollard T D 1998 Dynamic cross-linking by α -actinin determines the mechanical properties of actin filament networks *J. Biol. Chem.* **273** 9570–6
- [6] Sato M, Schwarz W H and Pollard T D 1987 Dependence of the mechanical properties of actin/alpha-actinin gels on deformation rate *Nature* **325** 828–30
- [7] Pollard T D and Borisy G G 2003 Cellular motility driven by assembly and disassembly of actin filaments *Cell* **112** 453–65
- [8] Fletcher D A and Theriot J A 2004 An introduction to cell motility for the physical scientist *Phys. Biol.* **1** T1–T10
- [9] Howard J and Hyman A A 2003 Dynamics and mechanics of the microtubule plus end *Nature* **422** 753–8
- [10] Yeung T *et al* 2005 Effects of substrate stiffness on cell morphology, cytoskeletal structure and adhesion *Cell Motil. Cytoskeleton* **60** 24–34
- [11] Discher D E, Janmey P and Wang Y-L 2005 Tissue cells feel and respond to the stiffness of their substrate *Science* **310** 1139–43
- [12] Guilak F *et al* 2009 Control of stem cell fate by physical interactions with the extracellular matrix *Cell Stem Cell* **5** 17–26
- [13] Fritsch A *et al* 2010 Are biomechanical changes necessary for tumour progression? *Nature Phys.* **6** 730–2
- [14] Merrill E W *et al* 1963 Rheology of human blood, near and at zero flow: effects of temperature and hematocrit level *Biophys. J.* **3** 199–213
- [15] Williamson J, Shanahan M and Hochmuth R 1975 The influence of temperature on red cell deformability *Blood* **46** 611–24

- [16] Hochmuth R M, Buxbaum K L and Evans E A 1980 Temperature dependence of the viscoelastic recovery of red cell membrane *Biophys. J.* **29** 177–82
- [17] Petersen N O, McConnaughey W B and Elson E L 1982 Dependence of locally measured cellular deformability on position on the cell, temperature and cytochalasin B *Proc. Natl Acad. Sci. USA* **79** 5327–31
- [18] Sunyer R, Trepas X, Fredberg J J, Farré R and Navajas D 2009 The temperature dependence of cell mechanics measured by atomic force microscopy *Phys. Biol.* **6** 025009
- [19] Rico F, Chu C, Abdulreda M H, Qin Y and Moy V T 2010 Temperature modulation of integrin-mediated cell adhesion *Biophys. J.* **99** 1387–96
- [20] Anson M 1992 Temperature dependence and Arrhenius activation energy of F-actin velocity generated *in vitro* by skeletal myosin *J. Mol. Biol.* **224** 1029–38
- [21] Kawaguchi K and Ishiwata S 2000 Temperature dependence of force, velocity and processivity of single Kinesin molecules *Biochem. Biophys. Res. Commun.* **272** 895–9
- [22] Zimmerle C T and Frieden C 1986 Effect of temperature on the mechanism of actin polymerization *Biochemistry* **25** 6432–8
- [23] Digel I, Kayser P and Artmann G M 2008 Molecular processes in biological thermosensation *J. Biophys.* **2008** 602870
- [24] Guck J, Ananthakrishnan R, Moon T J, Cunningham C C and Kaes J 2000 Optical deformability of soft biological dielectrics *Phys. Rev. Lett.* **84** 5451
- [25] Guck J *et al* 2005 Optical deformability as an inherent cell marker for testing malignant transformation and metastatic competence *Biophys. J.* **88** 3689–98
- [26] Lincoln B *et al* 2007 Reconfigurable microfluidic integration of a dual-beam laser trap with biomedical applications *Biomed. Microdevices* **9** 703–10
- [27] Ebert S, Travis K, Lincoln B and Guck J 2007 Fluorescence ratio thermometry in a microfluidic dual-beam laser trap *Opt. Express* **15** 15493–9
- [28] Wetzel F *et al* 2011 Single cell viability and impact of heating by laser absorption *Eur. Biophys. J.* **9** 1109–14
- [29] Gyger M *et al* 2011 Calcium imaging in the optical stretcher *Opt. Express* **19** 19212–22
- [30] Lou J, Finegan T, Mohsen P, Hatton T A and Laibinis P E 1999 Fluorescence-based thermometry: principles and applications *Rev. Anal. Chem.* **18** 235–84
- [31] Ferry J D 1980 *Viscoelastic Properties of Polymers* 3rd edn (New York: Wiley)
- [32] Schwarzl F and Staverman A 1952 Time–temperature dependence of linear viscoelastic behavior *J. Appl. Phys.* **23** 838–43
- [33] Maloney J M *et al* 2010 Mesenchymal stem cell mechanics from the attached to the suspended state *Biophys. J.* **99** 2479–87
- [34] Fabry B *et al* 2001 Scaling the microrheology of living cells *Phys. Rev. Lett.* **87** 148102
- [35] Trepas X *et al* 2007 Universal physical responses to stretch in the living cell *Nature* **447** 592–5
- [36] Wang J H, Robinson C V and Edelman I S 1953 Self-diffusion and structure of liquid water: III. Measurement of the self-diffusion of liquid water with H₂, H₃ and O₁₈ as Tracers *J. Am. Chem. Soc.* **75** 466–70
- [37] Krellen D W and Nijenhuis K 2009 *Properties of Polymers: Their Correlation with Chemical Structure; Their Numerical Estimation and Prediction from Additive Group Contributions* (Amsterdam: Elsevier) pp 533–45
- [38] Gaikwad A N, Choperena A, Painter P C and Lodge T P 2010 Restoring thermorheological simplicity in miscible polymer blends: how many hydrogen bonds are required? *Macromolecules* **43** 4814–21
- [39] Resch J, Keßner U and Stadler F 2011 Thermorheological behavior of polyethylene: a sensitive probe to molecular structure *Rheol. Acta* **50** 559–75
- [40] Song Chang W 1984 Effect of local hyperthermia on blood flow and microenvironment: a review *Cancer Res.* **44** (Suppl. 10) 4721s–30s
- [41] Uchida N, Kato H and Ishida T 1993 A model for cell killing by continuous heating *Med. Hypotheses* **41** 548–53

- [42] Wolff L, Fernandez P and Kroy K 2011 Inelastic mechanics of sticky biopolymer networks *New J. Phys.* **12** 053024
- [43] Markovitz H 1975 Superposition in rheology *J. Polym. Sci. Polym. Symp.* **50** 431–56
- [44] Scalley M L and Baker D 1997 Protein folding kinetics exhibit an Arrhenius temperature dependence when corrected for the temperature dependence of protein stability *Proc. Natl Acad. Sci. USA* **94** 10636–40
- [45] Salbreux G, Joanny J F, Prost J and Pullarkat P 2007 Shape oscillations of non-adhering fibroblast cells *Phys. Biol.* **4** 268–84
- [46] Nishiyama H *et al* 1997 A Glycine-rich RNA-binding protein mediating cold-inducible suppression of mammalian cell growth *J. Cell Biol.* **137** 899–908
- [47] Yeom M, Pendergast J S, Ohmiya Y and Yamazaki S 2010 Circadian-independent cell mitosis in immortalized fibroblasts *Proc. Natl Acad. Sci. USA* **107** 9665–70
- [48] Bull J and Vogt R 1979 Temperature-dependent sex determination in turtles. *Science* **206** 1186–8
- [49] Conover D O and Kynard B E 1981 Environmental sex determination: interaction of temperature and genotype in a fish *Science* **213** 577–9
- [50] Pullarkat P A, Fernández P A and Ott A 2007 Rheological properties of the Eukaryotic cell cytoskeleton *Phys. Rep.* **449** 29–53